Excitation of the $3^{1,3}D$ and $4^{1,3}F$ Levels of Helium by Direct Electron Impact, and $4^1P \rightarrow 4^{1,3}F$ Collisional Transfer*

R. J. Anderson, R. H. Hughes, and T. G. Norton†
Department of Physics, University of Arkansas, Fayetteville, Arkansas 72701
(Received 26 December 1968)

Excitation of the $3^{1,3}D$ and $4^{1,3}F$ levels of helium by electron impact has been studied by time-resolved spectroscopy of the $3^1D \rightarrow 2^1P$(λ6678 Å) and $3^3D \rightarrow 2^3P$(λ5876 Å) transitions. (Excitation of the 4^1F and 4^3F levels are observed as cascade components under time resolution.) Cross sections are estimated for the direct excitation of these levels by 38-, 50-, and 100-eV electron impact. Excitation of the $4F$ levels by direct electron impact are much larger than predicted by the Born approximation but much smaller than implied by previous experimental measurements. Direct excitation of the 3^1D and 4^1F by 100-eV electron impact is in excellent agreement and satisfactory agreement, respectively, with preliminary close-coupling approximation calculations. The collisional transfer $4^1P \rightarrow 4^3F$ is much smaller relative to the $4^1P \rightarrow 4^1F$ transfer than has previously been suggested.

I. INTRODUCTION

Theoretical cross-section calculations employing the Born and the Born-Oppenheimer approximations yield results which underestimate the excitation of the 3^1D and 3^3D levels by electron impact when compared with experiment.[1] This is the case even at energies where the Born approximation is expected to be valid. In order to make a valid comparison between experiment and theory, however, it is necessary to properly correct the experimental measurements for the effects of secondary excitation processes, such as cascade (radiative transfer from higher states).

Radiative transfer from F states that have been excited by direct electron impact can play an important role in populating the $3^{1,3}D$ levels, according to recent measurements of Jobe and St. John.[2] They obtained very large cross sections for the excitation of the $4F$ levels by electron impact. However, the measurement of F-level excitation requires care, since these levels are sensitive to the collisional transfer reaction, $n^1P \rightleftarrows nF$. This reaction has been previously studied by Kay and Hughes[3] using time-resolved spectroscopy, which is a powerful tool in the analysis of secondary excitation mechanisms. Employing this method, cascading levels can be identified by their characteristic lifetimes, and their contribution to the population of the level in question can be determined absolutely.

This paper describes an experiment in which excitation of the 3^1D, 3^3D, 4^1F, and 4^3F levels by electron impact is measured by applying time-resolved spectroscopy to the $3^1D \rightarrow 2^1P$ (λ6678 Å) and $3^3D \rightarrow 2^3P$ (λ5876 Å) transitions.

II. EXPERIMENT

The experimental apparatus is comprised of three basic components: (1) an excitation tube, vacuum system, and source of helium atoms; (2) an electron gun to provide a gated electron beam of controlled energy into a field free collision region; and (3) photometric equipment to detect and record the radiative decay of the excited atomic states as a function of time after cessation of electron excitation. A block diagram of the apparatus is shown in Fig. 1. Helium gas is allowed to enter the excitation tube through a cooled trap containing charcoal granules. The excitation tube is sealed off from the vacuum system, and the helium gas pressure is determined by means of a trapped McLeod gauge.

The cathode and grid structure of a 6EM5 beam-power pentode tube are used as an electron gun to provide a sheet beam of monoenergetic electrons. The gun is biased to cut off by application of a negative dc potential on the control grid. A positive pulse, sufficiently large to cause the

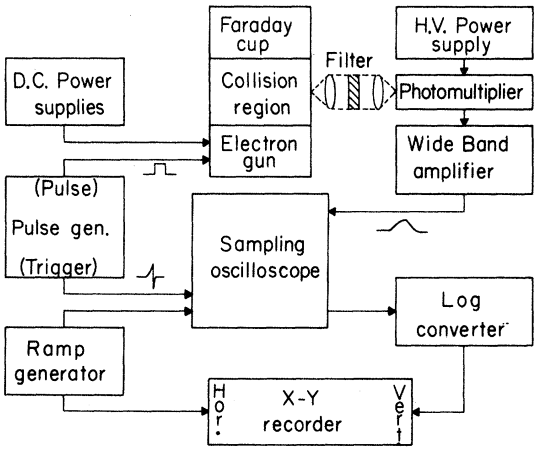

FIG. 1. Block diagram of experimental apparatus.

tube to conduct, is repeatedly applied to the control grid at a rate of 50 kHz, and produces a gated electron beam with cut off times of the order of 7 nsec. The pulse is 1 μsec long, an interval which we find experimentally to be of sufficient length to allow equilibrium of the excited state population to occur. The electron beam passes through a field free collision region and is collected in a deep Faraday cup, where it is monitored.

The resulting collisional radiation passes out of the excitation tube, at right angles to the electron beam direction, through a quartz window which is placed immediately adjacent to the electron beam. The collisional radiation corresponding to either the $3\,^1D \rightarrow 2\,^1P$ (λ6678 Å) or the $3\,^3D \rightarrow 2\,^3P$ (λ5876 Å) transition is isolated by an appropriate interference filter and is then detected by a fast-response photomultiplier tube operated in a dc mode. The phototube produces a 50-kHz electrical signal corresponding to the repeated decays of the collisional radiation. The signal is amplified by a wide band amplifier and is then directed to a sampling oscilloscope. The oscilloscope generates a strobe pulse which opens a sampling gate of approximately 0.35-nsec duration and admits the photomultiplier signal to its vertical deflection plates. A sample of the signal is taken in a time which is short when compared with the lifetime of the excited atomic state which makes the sample a good approximation of the instantaneous signal at that time. The sampling gate is then slowly advanced with respect to the beginning of each decay curve by a linear ramp; thus the oscilloscope recreates a single decay curve which is the composite of approximately 10^7 actual decay curves. The electronically averaged oscilloscope signal is directed to a logarithmic converter, whose output is displayed on the vertical axis of an x-y recorder, while the linear ramp is used to advance the x axis. The resulting trace is a plot of the logarithm of intensity versus time after the cessation of electron excitation. Absolute calibration of the time axis is achieved by monitoring a signal of known frequency with the sampling system. The minimum response time of the total detection system was determined to be approximately 3 nsec by employing a method similar to that described by Pendleton.[4]

The present investigation has used an imprisonment shield to reduce the population of the $n\,^1P$

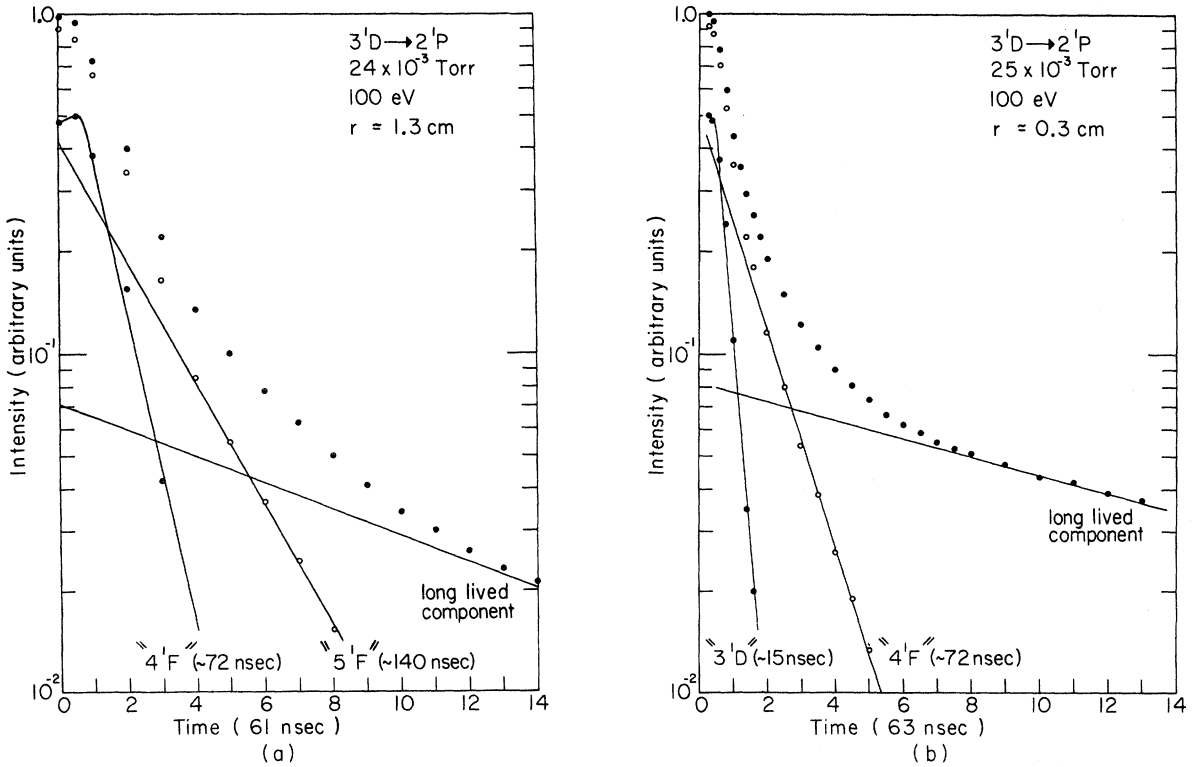

FIG. 2. Decay modes present in the $3\,^1D \rightarrow 2\,^1P$($\lambda$6678 Å) transition at approximately 25-mTorr helium pressure and 100-eV electron-impact energy; (a) without the imprisonment shield, (b) with the imprisonment shield. The decay modes are obtained by applying successive subtractions of the long-lived component and various "nF" decay curves to the original data points. The decay constant of each mode is measured and is identified as that belonging to a particular level through comparison with the theoretical transition probabilities reported by A. H. Gabriel and D. W. O. Heddle [Proc. Roy. Soc. (London), Ser. A 258, 124 (1960)].

levels produced by radiative trapping of $n\,^1P \rightarrow 1\,^1S$ resonance radiation. The shield forms a three-sided rectangular cavity, whose dimensions (3 cm long, 0.4 cm wide, 4 cm high) are approximately those of the electron beam and in which the collision processes under investigation occur. Absorption of resonance photons by the walls of the shield becomes an important loss process which competes with the radiative trapping process. The net effect is to decrease the experimentally measured effective imprisonment radius of the apparatus[3] (e.g., $r \approx 0.3$ cm with the shield in use versus $r \approx 1.3$ cm without the shield). Figure 2 compares the decay modes present in the $3\,^1D \rightarrow 2\,^1P$ (λ6678 Å) transitions without the imprisonment shield [Fig. 2(a)] and with the imprisonment shield [Fig. 2(b)] under nearly identical excitation conditions of electron-impact energy and pressure, 100 eV and about 25 mTorr, respectively. The striking feature in Fig. 2(b) is the suppression of the long-lived cascade components relative to directly excited 15 nsec $3\,^1D$ decay by the action of the shield. The directly excited $3\,^1D$ decay component cannot even be detected without the shield [Fig. 2(a)]. The shield reduces the population of $n\,^1P$ levels and hence suppresses the $n\,^1P \rightarrow n\,^1F$ collisional reaction which contributes heavy F-level cascade to $3\,^1D$ at this energy and pressure.

III. TREATMENT OF DATA

Kay and Hughes[3] have shown how to treat cascade events in time-resolved spectroscopy. Using their example, consider the case where state k cascades to state j and the excitation pulse (the electron beam in this case) has established excitation equilibrium prior to being turned off at a time $t = 0$. The rate equation for the state, $t > 0$, is given by

$$\dot{n}_j = n_k{}^0 A_{kj}\, e^{-t/\tau_k} - n_j/\tau_j\,, \tag{1}$$

where n_j is the density of atoms in state j, $n_k{}^0$ is the density of atoms in state k at $t = 0$, A_{kj} is the transition probability $k \rightarrow j$, and τ_k and τ_j are the lifetimes of states k and j, respectively.

The solution to this equation is

$$n_j = \beta e^{-t/\tau_j} + \gamma_k e^{-t/\tau_k}\,, \tag{2}$$

where $\beta = n_j{}^0 - \gamma_k$,

$$\gamma_k = n_k{}^0 A_{kj}\, \tau_j (1 - \tau_j/\tau_k)^{-1},$$

and $n_j{}^0$ is density of atoms in state j at $t = 0$.

Thus if $\tau_k > \tau_j$, a semilog plot of n_j versus t would show two characteristic decay modes having positive initial intercepts at $t = 0$ of β and γ_k.

Since at $t = 0$, $n_j{}^0 = n_j^* + \tau_j n_k{}^0 A_{kj}$, where n_j^* is the density of atoms placed in state j by direct electron impact, then

$$n_j^* = \beta + \gamma_k \tau_j / \tau_k\,. \tag{3}$$

Pertinent cross sections are defined through the following customary equations:

$$n_j{}^0 = \Phi\rho\tau_j Q_j'\,, \quad n_j^* = \Phi\rho\tau_j Q_j\,,$$

and $$n_k{}^0 = \Phi\rho\tau_k Q_k\,,$$

where Φ is electron flux, ρ is the gas density, Q_j' is the apparent cross section for populating j which would be measured by a dc electron-beam experiment, Q_j is the cross section for populating j by direct electron impact, and Q_k is the cross section for populating k by direct electron impact (neglecting radiative cascade into the kth state). Defining $f_\beta = \beta/n_j{}^0$ and $f_k = \gamma_k/n_j{}^0$ which are the fractions of the total decay having intercepts β and γ_k, respectively, then $f_\beta + f_k = 1$.

Letting k now represent several cascading states, it follows that

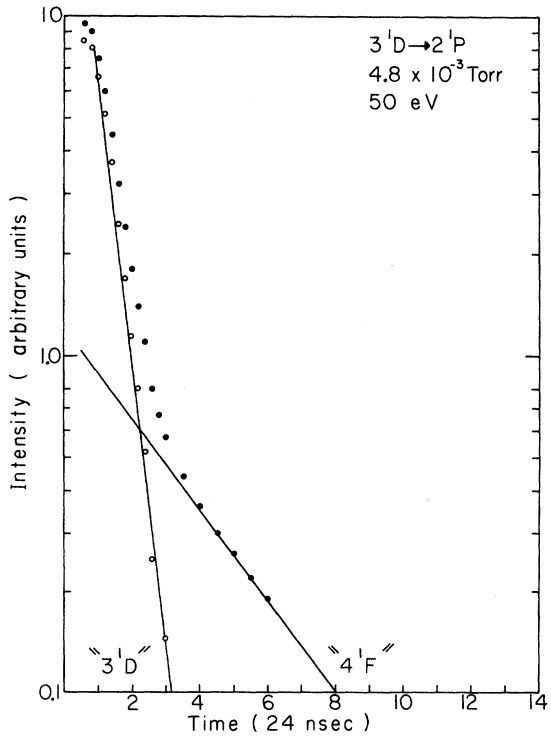

FIG. 3. Typical $3\,^1D \rightarrow 2\,^1P$($\lambda$6678 Å) decay scheme taken at 4.8-mTorr helium pressure and 50-eV electron-impact energy. The $3\,^1D$ (15 nsec) and $4\,^1F$ (72 nsec) decay modes are identified.

$$Q_j = Q_j'(f_\beta + \textstyle\sum_k f_k \tau_j/\tau_k) \quad (4)$$

and $f_\beta + \sum_k f_k = 1$. In addition,

$$Q_k = f_k(1 - \tau_j/\tau_k)(A_{kj}\tau_k)^{-1} Q_j'. \quad (5)$$

IV. RESULTS AND DISCUSSION

A. Excitation Cross Sections

A representative low-pressure decay curve corresponding to the $3\,^1D \rightarrow 2\,^1P$ (λ6678 Å) transition excited by 50-eV electron impact is shown in Fig. 3. Only the $3\,^1D$ (15 nsec) and $4\,^1F$ (72 nsec) decay modes could be detected in each of the low-pressure 6678 Å total decays. The $n\,^1F$ ($n>4$) decay modes are undoubtedly present but are estimated to represent 2% or less of the total decays and cannot be detected. Examination of the representative curve indicates that the $3\,^1D$ level is primarily populated by direct electron impact; i.e., the $3\,^1D$ decay mode comprises ~90% of the total population.

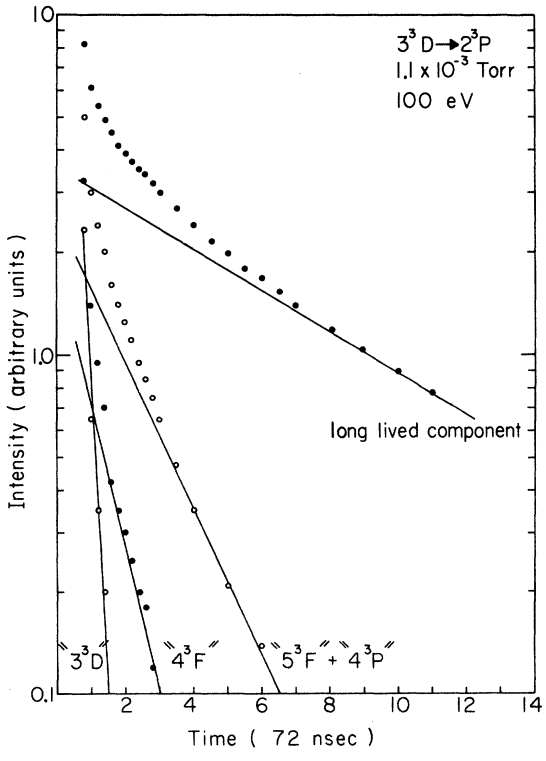

FIG. 4. Typical $3\,^3D \rightarrow 2\,^3P$(λ5876 Å) decay scheme taken at 1.1-mTorr helium pressure and 100-eV electron-impact energy. The total decay is resolved into four separate decay modes corresponding to the contributions of the $3\,^3D$ (15 nsec), $4\,^3F$ (72 nsec) and $5\,^3F + 4\,^3P$ (~140 nsec) levels; and a long-lived component (~515 nsec).

Figure 4 shows a similar low-pressure curve corresponding to the $3\,^3D \rightarrow 2\,^3P$ (λ5876 Å) transition excited by 100-eV electron impact. In general the 5876 Å total decay shows considerably more structure with only 50 to 65% of the total decay being attributed to the sum of the $3\,^3D$ and $4\,^3F$ decay modes. Cascade from the $n\,^3P$ and $n\,^3F$ states are the main contributors to the remainder. The ^3P and ^3F states cannot be individually identified because of the similarities in radiative lifetimes. For example, the $4\,^3P$ and $5\,^3F$ levels, both heavy cascade contributors to the total $3\,^3D$ population, have nearly identical radiative lifetimes of about 140 nsec.

Figure 5 is a plot of the fraction of the total $3\,^1D \rightarrow 2\,^1P$ decay having the $3\,^1D$ radiative lifetime (15 nsec) and $4\,^1F$ radiative lifetime (72 nsec) as a function of pressure for 100-eV electron-impact energy. The fractions were obtained from decay data similar to that displayed in Fig. 3. Each point represents the average of from 3 to 10 fractions obtained through analysis of individual decay curves. The error limits placed on each fraction are representative of both data reproducibility and errors introduced through the analysis of each decay curve. This plot markedly shows the effect of the collisional transfer as the pressure increases. The fraction of the total decay associated with the $3\,^1D$ lifetime rapidly decreases with the pressure while that associated with the $4\,^1F$ lifetime increases. This indicates that there exists a pressure-dependent mechanism which is populating the $4\,^1F$ level.

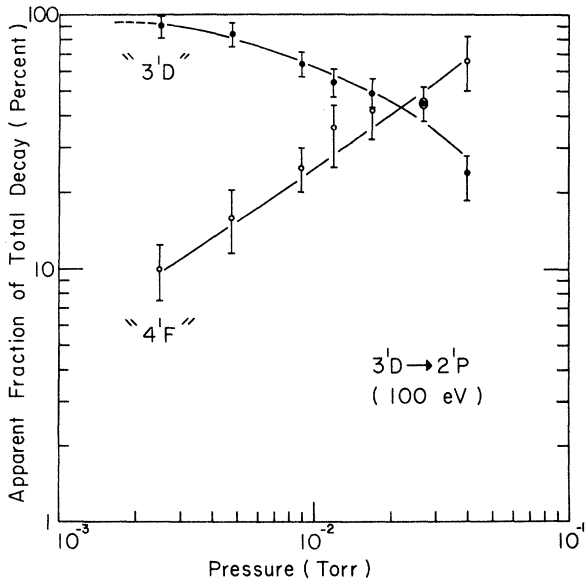

FIG. 5. Apparent fractions of total $3\,^1D \rightarrow 2\,^1P$ decay corresponding to the $3\,^1D$ (15 nsec) and $4\,^1F$ (72 nsec) lifetimes as a function of pressure at 100-eV electron-impact energy.

Furthermore, our work indicates that the efficiency of this mechanism is increasing with the electron-impact energy. This type of dependency is a characteristic of the $4\,^1P \rightarrow 4\,^1F$ transfer mechanism.

In order to obtain information concerning the excitation of the $3\,^1D$ and $4\,^1F$ levels by direct electron impact, it is necessary to decrease the pressure to the point where the collisional transfer mechanism becomes unimportant. When this point is reached, the fractions will become independent of the pressure. The plots show that the fractions have become constant at the lowest pressures. These fractions are inserted into Eqs. (4) and (5) along with the apparent $3\,^1D$ cross section (Q_j') values from Ref. 1 to determine the $3\,^1D$ and $4\,^1F$ cross sections for direct electron impact.

The same procedure is applied to obtain the $3\,^3D$ and $4\,^3F$ cross sections for direct electron impact. Figures 6 and 7 are plots of the fractions of the total $3\,^3D \rightarrow 2\,^3P$ decay having the $3\,^3D$ radiative lifetime (15 nsec) and $4\,^3F$ radiative lifetime (72 nsec) as a function of pressure. Each point was obtained in a manner similar to that described for the singlet case. However, for 100-eV electron impact we were not able to reach the pressure-independent region and thus are forced to extrapolate. Figure 7 shows our extrapolation of the curves.

The results of these procedures are displayed in Table I where the cross sections for directly exciting the $3\,^1D$, $3\,^3D$, $4\,^1F$ and $4\,^3F$ are tabulated along with the apparent cross section of Ref. 1.

At these energies, little cascade is to be found in the low-pressure $3\,^1D \rightarrow 2\,^1P$ transition; hence, the $3\,^1D \rightarrow 2\,^1P$ optical cross section needs only a small correction in order to obtain the $3\,^1D$ excitation cross section. The close-coupling approximation has been used by Lin and Chung to calculate the $3\,^1D$ excitation at 100 eV.[5] They obtain a preliminary value of 22×10^{-20} cm^2 which is in excellent agreement with the cascade corrected value in Table I. Using the same method, Lin and Chung have also calculated the excitation cross section for the $4\,^1F$ level at 100 eV. They obtain a preliminary vlaue of 0.5×10^{-20} cm^2 as compared with the Born value of 0.014 $\times 10^{-20}$ cm^2. The larger value is in reasonable agreement with our value in Table I.[6]

Considerable cascade is observed in the $3\,^3D \rightarrow 2\,^3P$ transition; hence the $3\,^3D \rightarrow 2\,^3P$ low-pressure optical cross section must be heavily corrected to obtain the cross section for direct excitation of the $3\,^3D$ level. In view of the apparent success of the close-coupling approximation in predicting the $3\,^1D$ and $4\,^1F$ cross sections, it would be interesting to compare the results of such calculations for the $3\,^3D$ and the $4\,^3F$, when electron exchange is included, with the corresponding experimental values. Optical cross sections have been obtained by St. John and Jobe[2] for $4F$ excitation via observation of the $4F \rightarrow 3D$ transitions (unresolved triplet and singlet) occurring at about 18 695 Å. Their reported cross sections, however, are considerably

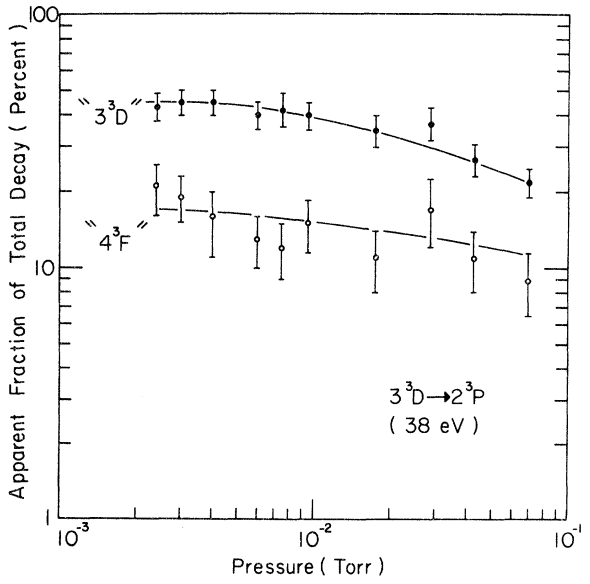

FIG. 6. Apparent fractions of total $3\,^3D \rightarrow 2\,^3P$ decay corresponding to the $3\,^3D$ (15 nsec) and $4\,^3F$ (72 nsec) lifetimes as a function of pressure at 38-eV electron-impact energy.

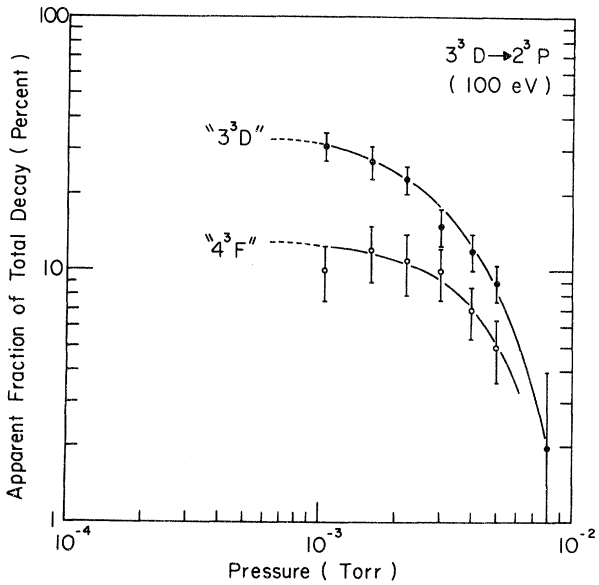

FIG. 7. Apparent fractions of total $3\,^3D \rightarrow 2\,^3P$ decay corresponding to the $3\,^3D$ (15 nsec) and $4\,^3F$ (72 nsec) lifetimes as a function of pressure at 100-eV electron-impact energy.

TABLE I. Estimates of cross sections for direct electron impact in units of 10^{-20} cm^2. Listed uncertainties are relative to the experimental measurements of this paper only.

	$Q'(3\,^1D)$ [a]	$Q'(3\,^3D)$ [a]	$Q(3\,^1D)$	$Q(3\,^3D)$	$Q(4\,^1F)$	$Q(4\,^3F)$
38 eV	39	30	35 ± 5	15 ± 2	4.3 ± 1.2	4.1 ± 1.2
50 eV	42	18	39 ± 4	8.6 ± 0.9	2.7 ± 0.7	2.0 ± 0.5
100 eV	24	4.5	23 ± 3	1.7 ± 0.2	1.1 ± 0.5	0.5 ± 0.2

[a]Apparent cross sections from Ref. 1.

larger than ours – an order of magnitude larger at 100 eV. Their larger measurements can be reconciled with the results of this experiment under the following two assumptions: (1) Their infrared measurements used an absolute calibration scale which gave a higher cross section by a factor of about 1.8. (2) Their measurements were carried out at too high a pressure (8 mTorr) to neglect collisional transfer.

B. Excitation Transfer

Kay and Hughes[3] measured the total collisional transfer cross sections in the $n\,^1P \rightarrow nF$ reaction for $n=4$, 5, and 6. They also attempted to determine the branching of the $n\,^1P$ collisional transfer to the $n\,^1F$ and $n\,^3F$ levels on the assumption that the direct excitation of ^1F and ^3F levels by electron impact could be neglected at 34 mTorr. The present experiment shows this to be a poor assumption. It of course has no effect on their total transfer measurements but it does invalidate their branching ratios (Table II. Ref. 3).

In order to compare the magnitude of the $n\,^1P$ transfer with $n\,^3F$ states relative to $n\,^1F$ states, it was necessary to determine the optical efficiency of our apparatus at 5876 Å relative to 6678 Å. We observed the excitation for 50-eV electron impact at low pressures with the imprisonment shield in place. Under these conditions, we were assured that we were observing only direct excitation by electron impact. The photomultiplier current was recorded first for 5876 Å and then 6678 Å radiation while the pressure and electron-beam current were held constant. The relative optical efficiency was determined by using the ratio of these photomultiplier signals, and the corresponding relative cross sections for direct excitation from Ref. 1.

Kay and Hughes[3] treat the collisionally coupled P and F states and show that the decay of the P and F states will exhibit the characteristics of both systems. However, the collision frequencies and radiative transition probabilities are such that one can usually approximate the F-state decays by single exponentials. Figures 8 and 9 show the analysis of 100 eV, 100-mTorr decay curves obtained with the imprisonment shield removed. Notable features of these decay curves include the heavy contribution of the $4F$ decay in the $3\,^1D \rightarrow 2\,^1P$ radiation and the lack of $4F$ decay in the $3\,^3D \rightarrow 2\,^3P$ radiation. They also exhibit a decay mode that may be attributed primarily to a combination of the $5F$ and $6F$ levels plus a smaller amount of cascade, from higher levels.

A study of pressure dependency of the $4F$ components in the $3\,^1D \rightarrow 2\,^1P$ and $3\,^3D \rightarrow 2\,^3P$ transitions has shown that very little of the $4\,^1P \rightarrow 4F$ transfer goes to the $4\,^3F$ level and, in fact, it appears to be zero within experimental error, with at most 10% going to the $4\,^3F$. This is consistent with the spin conservation rule and is consistent with the $4\,^3F$ findings in Ref. 3 which can be attributed entirely to direct excitation. When the data of Ref. 3 for $3\,^3D$ excitation at 38 eV and a pressure of 34 mTorr is properly calibrated to give our cross section of 15×10^{-20} cm^2

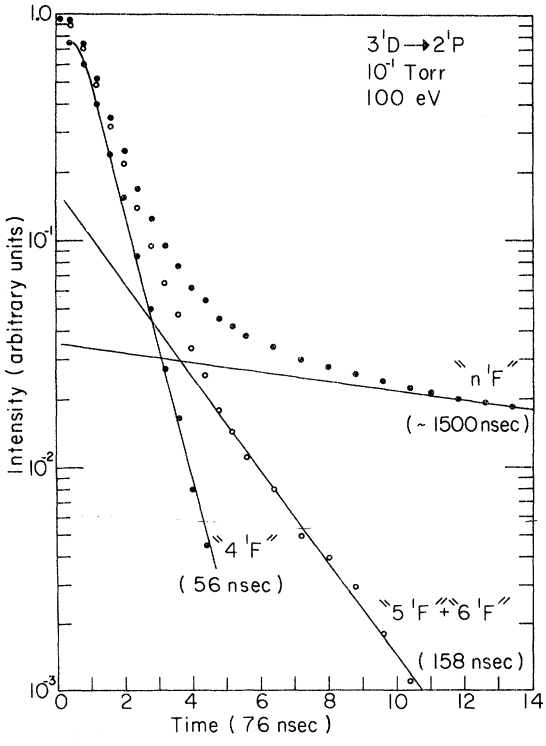

FIG. 8. Decay scheme of the $3\,^1D \rightarrow 2\,^1P$(λ6678 Å) transition obtained with the imprisonment shield removed at 100-mTorr helium pressure and 100-eV electron-impact energy.

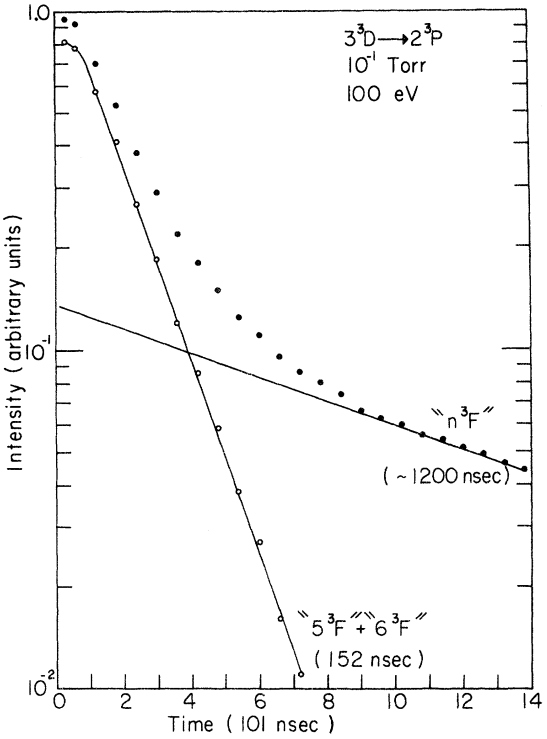

FIG. 9. Decay scheme of the $3\,^3D \rightarrow 2\,^3P(\lambda 5876\,\text{Å})$ transition obtained with the imprisonment shield removed at 100-mTorr helium pressure and 100-eV electron-impact energy.

for the direct $3\,^3D$ excitation, then the apparent $4\,^3F$ cross section becomes $(5 \pm 3) \times 10^{-20}$ cm^2. This is our value for the direct $4\,^3F$ cross section, $(4.1 \pm 1.2) \times 10^{-20}$ cm^2, within experimental error.

The model of $n\,^1P \rightarrow nF$ transfer used by St. John and Nee[7] considerably underestimates the collisional transfer contribution to the $3\,^1D$ apparent cross section. They would estimate the ratio of apparent $3\,^1D$ to $3\,^3D$ cross sections to be about 1.4 as compared with our experimental value of about 2.8 at 100 mTorr. This underestimate comes about because their model (and that used by Ref. 3) shares the $4\,^1F$ collisional excitation with $4\,^3F$ level. At 100 mTorr the most important single collisional process is at the $n = 4$ level; hence a model in which the $4\,^1P$ transfer is assumed to transfer an appreciable amount to the $4\,^3F$ will underestimate the apparent $3\,^1D$ cross section.

We have gained several bits of information necessary for the construction of the $nP \rightarrow nF$ transfer model. These include the knowledge that $4\,^1P \rightarrow 4\,^3F$ transfer can be neglected and a reasonable knowledge of the apparent $3\,^1D$ cross sections at high pressures. We, therefore, can compare again the predictions of the excitation transfer model with experiment.

Table II shows the result of these comparisons. Since we cannot confidently separate out the $5F$ and $6F$ components in our high-pressure decay analyses, we simply use the sum of the two in our comparisons. The apparent $3\,^3D$ cross section at 100 mTorr is obtained by interpolating the $3\,^3D$ measurements of St. John[7] between 63 and 130 mTorr, and the $Q'(3\,^1D)$ value is obtained by multiplying the $Q'(3\,^3D)$ value by our experimental ratio of 2.8. We used $Q'(3\,^3D) = 60 \times 10^{-20}$ cm^2 and $Q'(3\,^1D) = 170 \times 10^{-20}$ cm^2 as "experimental" values.

The calculated values used the transfer cross sections of Kay and Hughes[3] for $n = 4$, $n = 5$, and $n = 6$. For $n > 6$ the cascade contribution is estimated using the extrapolations of Ref. 3. At a pressure of 100 mTorr the $n > 6$ transfer is not particularly important. The cascade contributions to the $3D$ apparent cross sections are expressed as fractions of the $4\,^1P$ direct cross section. The direct $4\,^1P$ cross section is a convenient cross section unit since the transfer model uses a n^{-3} scaling to estimate the direct $n\,^1P$ excitation cross sections for $n > 4$. The experimental values are also presented relative to the $4\,^1P$ direct excitation cross section for comparison purposes. The experimental values use the $4\,^1P$ cross section of Ref. 1, which seems a reasonable reference since all of our measurements are relative to the University of Oklahoma's measurements.

The calculated contributions are each about 22% lower than the "experimental" values. The agreement is certainly satisfactory in view of all the extrapolations and experimental uncertainties. It is difficult to estimate the uncertainties since we rely on another laboratory's measurements.

It is easily seen that the $4F$ cross-section measurements of Jobe and St. John could have been affected by collisional transfer. At 8 mTorr and using an imprisonment radius of 1.3, the model predicts 4% of the $4\,^1P$ direct excitation will go to the $4F$ levels. Considering the size of the $Q(4\,^1P)$ at 100 eV, this is an appreciable amount.

The fact that there is little $4\,^1P \rightarrow 4\,^3F$ transfer

TABLE II. Estimated cascade contribution to the $3D$ levels from $n\,^1P \rightarrow nF$ transfer at 100 mTorr in units of the $4\,^1P$ direct cross section. Calculated values use an imprisonment radius of 1.3 cm. Experimental values are relative to $Q(4\,^1P) = 160 \times 10^{-20}$ cm^2 (Ref. 1).

		$4F$	$5F + 6F$	$\sum nF$ $(n > 6)$
Calculated		0.51	0.40	0.09
Experiment	^3F	0	0.30	0.07
	^1F	0.64	0.24	0.03
Sum		0.64	0.54	0.10

would seem to indicate that the spin conservation rule is still applicable for this reaction. There is evidence, however, that there is breakdown in the LS coupling scheme for the $4F$ states. Abrams and Wolga[8] have measured considerable transfer in the case of $4\,^3F \rightarrow 4\,^1D$ relative to $4\,^3F \rightarrow 4\,^3D$. This of course is a different reaction. A glance at estimates of the spin-orbit interaction compared with the electrostatic repulsion interaction[9] shows that $4P$ is a good LS coupling term, $4D$ is poorer while $4F$ is the poorest. Thus the reaction, $4\,^3F \rightarrow 4\,^1D$, involves the pair of collision partners least likely to obey the spin conservation rules. A further consideration is that $4\,^1P$, $4\,^3F$ energy separation is over 6 times larger than the $4\,^1D$, $4\,^3F$ separation and thus the $4\,^1D$, $4\,^3F$ collision represents a nearer resonance reaction; however, both separations are smaller than thermal energies.

---

*Supported by the National Science Foundation.

†National Defense Education Act Title IV Predoctoral Fellow.

[1]R. M. St. John, F. L. Miller, and C. C. Lin, Phys. Rev. 134, A888 (1964).

[2]J. D. Jobe and R. M. St. John, J. Opt. Soc. Am. 57, 1449 (1967).

[3]R. B. Kay and R. H. Hughes, Phys. Rev. 154, 61 (1967).

[4]W. R. Pendleton, Rev. Sci. Instr. 36, 1645 (1965).

[5]S. Chung and C. C. Lin, Bull. Am. Phys. Soc. 13, 214 (1968).

[6]However, it is to be noted that the present experimental measurements are relative and that the resulting absolute direct excitation cross sections are dependent upon the values of the absolute apparent cross sections to which the relative data are normalized. At present there exist several sources of absolute excitation cross-section data, e.g., see B. L. Moiseiwitsch and S. J. Smith, Rev. Mod. Phys. 40, 238 (1968).

[7]R. M. St. John and T. Nee, J. Opt. Soc. Am. 55, 426 (1965).

[8]R. L. Abrams and G. J. Wolga, Phys. Rev. Letters 19, 1411 (1967).

[9]C. C. Lin and R. G. Fowler, Ann. Phys. (N.Y.) 15, 461 (1961).

PHYSICAL REVIEW VOLUME 181, NUMBER 1 5 MAY 1969

Generalized Oscillator Strengths of the Helium Atom. II. Transitions from the Metastable States*

Yong-Ki Kim and Mitio Inokuti
Argonne National Laboratory, Argonne, Illinois 60439

(Received 13 January 1969)

The generalized oscillator strengths for the transitions $2^1S \rightarrow 2^1P$, 3^1S, 3^1P, 3^1D, 4^1P, and $2^3S \rightarrow 2^3P$, 3^3S, 3^3P, 3^3D, 4^3P of He are computed from the Weiss correlated wave functions of the Hylleraas type. The results from two alternative formulas, corresponding to the "length" and "velocity" formulas in the optical limit, agree with each other within a few percent for moderate values of the momentum transfer. The first Born excitation cross sections for the above-mentioned transitions by charged-particle impact are also presented.

1. INTRODUCTION

Although the metastable 2^1S and 2^3S states of the helium atom play important roles in various gaseous phenomena as unique species by virtue of their long radiative lifetimes[1,2] and great reactivity,[3] current information on the inelastic scattering of charged particles by the metastable He atoms is quite limited.[4–7] We have, therefore, extended our earlier work on some transitions from the ground state[8] to include the generalized oscillator strengths for the $2^1S \rightarrow 2^1P$, 3^1S, 3^1P, 3^1D, 4^1P and $2^3S \rightarrow 2^3P$, 3^3S, 3^3P, 3^3D, 4^3P excitations. The Born cross sections[8,9] for the excitations by charged-particle impact are also presented.

We have used correlated wave functions by Weiss[10] as before, and we believe our results to